Large-scale Structures and their Role in Solar Activity
ASP Conference Series, Vol. 346, 2005
K. Sankarasubramanian, Matt Penn, and Alexei Pevtsov

On Magnetic Structures of Solar Active Regions and Geomagnetic Storms

Y. Liu
W. W. Hansen Experimental Physics Laboratory, Stanford University, Stanford, CA94305-4085

Abstract. In this paper, we investigate possible relationship between magnetic configurations of active regions and geomagnetic storms. Three active regions have been analyzed using various observational data and modelings. Each one was observed to be associated with multiple full halo coronal mass ejections (CMEs). This study demonstrates that, although the full halo CMEs were originated from the same active region, their geoeffectiveness can be different, depending on the magnetic configurations involved actually in the corresponding flare activities. This seems to suggest that it is the magnetic fields involved in the events but not the whole active region determine whether or not the events are geoeffective. It may suggest a way for geomagnetic storm prediction.

1. Introduction

It is generally believed that long intervals of large southward interplanetary magnetic field are one of the primary causes of intense geomagnetic disturbances, and the solar sources of such geoeffective solar wind structures are CMEs (Webb et al. 2001, and references therein). On significantly different spatial scales, flares usually occur within active regions, showing disturbances within localized areas, while CMEs are believed to be large scale or even global phenomena, related to large-scale solar magnetic fields. Even though, evidence has shown that at least some CMEs are associated with flares (see, e.g., Zhang et al. 2001). This suggests that magnetic field may serve as a link between flares, CMEs and geomagnetic storms. As flares usually occur in active regions, it is natural to ask if configurations of magnetic fields of active regions are an essential factor to determine whether or not the related events are geoeffective.

Actually, several studies were conducted recently to investigate such relationships. From *Yohkoh* X-ray images and a coronal flux rope model, Titov & Demoulin, (1999) and Pevtsov & Canfield (2001) analyzed geomagnetic events temporally associated with eruptions of active regions with coronal X-ray sigmoids in the period from 1991 to 1998. They found that eruptions with a southern leading magnetic field associated with stronger geomagnetic storms, but those with a northern leading field associated with more storms. They also found an increase of strong geomagnetic storms after 1996 (the solar minimum), which cannot be described reasonably by the scenario that the large-scale dipole field determines geoeffectiveness (see, e.g. Crooker 2000, and the references therein). They thus suggest that the magnetic structure of individual active regions play a role in geomagnetic events, but their geoeffectiveness is complicated by asymmetries in the leading and following magnetic field and density. Leamon, Canfield

and Pevtsov (2002) further this work by using a rather larger sample in the period from 1991 to 2000. They found that the leading fields in magnetic clouds weakly show a solar cycle based correlation, implying that the toroidal fields of individual active regions are related directly to their heliospheric structure. But they also showed inconsistence of helicity signs between active regions and their related magnetic clouds. On the other hand, Yurchyshyn et al. (2001) proposed an operational scheme for geoeffectiveness forecast based on magnetic helicity and configuration of eruptive filaments.

Though interest has been increasing in understanding the role of solar active regions for occurrence of geomagnetic storms, and evidence has already been presented to demonstrate weakly a magnetic link, it is still far from establishing a certain correlation between them. In other words, it is unclear so far what kinds of active regions are likely to cause geomagnetic storms. To investigate this question, in this paper, we study magnetic configurations of active regions which associate with multiple full halo CMEs. The basic thought for this task is that if magnetic configurations of active regions are a key factor to determine occurrence of geomagnetic storms, the full halo CMEs originated from the same active region should show similar geoeffectiveness.

This paper is organized as follow. In section 2, we give a list of active regions which will be studied in this research. Each active region is associated with multiple flare-associated full halo CMEs. Their geoeffectiveness is also identified unambiguously. This list is based on two existing databases. One is the Table 2 in Zhang et al. (2003). This table contains the geomagnetic-storm-related full halo CMEs from 1996 to 2000. Solar source regions of those CMEs are identified carefully using observations such as *SOHO/EIT*. The other is from Webb et al. (2004), who study all 134 full halo CMEs observed by LASCO from 1996 to 2000. A geomagnetic storm in that study is defined by Dst $<$ -50 nT. Solar disk regions for those CMEs are determined by observations, such as Hα data and EIT images. In section 3, we will analyze magnetic configurations of the active regions, and explore relationship of those configurations and geoeffectiveness. We summarize our results in Section 4, together with a brief discussion.

2. Active Regions with Multiple Halo CMEs

We search for active regions from the databases mentioned in previous Section. The criteria for this selection are (1) the active regions are associated with multiple full halo CMEs; (2) each CME is associated with a solar flare; and (3) its geoeffectiveness is identified unambiguously. Three active regions are finally chosen, and the corresponding information is presented in Table 1. The first column of this table is event number. The characters w and z denote the original sources of the events. The w represents that the event is from Webb et al (2004), while the z means the event is from Zhang et al (2003). The 2nd – 4th columns are flare, flare date and flare time, respectively. Here, the flare time represents the flare start time. Each flare is identified to be associated with a full halo CME. The 5th and 6th columns are the solar disk regions and their disk coordinates. The related geomagnetic storms are presented in the last column.

Table 1. Active Regions with Multiple Halo CMEs & their Geoeffectiveness

Eruption Number	Flare	Date (mm/dd/yy)	Time[a] (UT)	Source (AR)	Coordinate (degree)	Storm Dst (nT)
1[z]	M4.2	11/03/97	10:18	8100	S20W15	–
2[w,z]	X2.1/2B	11/04/97	05:54	8100	S14W33	-110
3[w]	X9.4/2B	11/06/97	11:22	8100	S18W63	-54
4[w,z]	C5.2/SF	11/04/98	03:14	8375	N17E01	-81
5[w]	C5.4/SF	11/05/98	02:59	8375	N19W11	-149
6[w,z]	M8.4/2B	11/05/98	18:31	8375	N22W18	-142
7[w]	X2.3/3B	06/06/00	12:06	9026	N20E18	-80
8[w]	X1.2/3B	06/07/00	15:04	9026	N23E03	-56
9[w]	M5.2/3B	06/10/00	16:37	9026	N22W38	–

[a] Flare start time from *SGD*.

[w] Event identified by Webb et al. (2004).

[z] Event identified by Zhang et al. (2003).

3. Results

Flares shown in *SOHO* and *YOHKOH* images are aligned to the relative magnetograms in order to study magnetic configurations associated with them. The alignment was done basically using the *IDL* map softwares in the Solar SoftWare (SSW) written by D. Zarro.

3.1. Active Region AR8100

Active region AR8100 produced three flares that were associated with full halo CMEs: M4.2 occurred at 10:18UT of November 3, X2.1/2B at 05:54UT of November 4, and X9.4/2B flare at 11:22UT of November 6 (see Table 1). The locations of the flares are marked respectively by 'F1', 'F2' and 'F3' on the corresponding magnetograms in Figure 1. It is seen that the X2.1/2B and X9.4/2B flares occurred at the same location while the M4.2 flare occurred somewhere else.

Magnetic field observation seems to suggest that the magnetic fields involved in the M4.2 flare are different with those in the X2.1/2B and X9.4/2B flares. The M4.2 flare appears to be associated with an elongated negative magnetic feature. An MDI magnetogram movie clearly shows that this feature is actually an emerging flux region first shown in the November 03 08:03:03 magnetogram. Flares X2.1/2B and X9.4/2B, on the other hand, were associated with a feature with positive sign of magnetic polarity. This feature, first seen in the November 2 22:24:04 magnetogram, is likely to be another emerging flux region. It continued emerging and developing in the following days.

Magnetic structure of this active region can be well represented by extrapolated non-linear force-free magnetic fields (Liu et al. 2002). The *Yohkoh* Soft X-ray patterns above this region were reproduced successfully by the non-linear force-free field calculation. This calculation was carried out based on a bound-

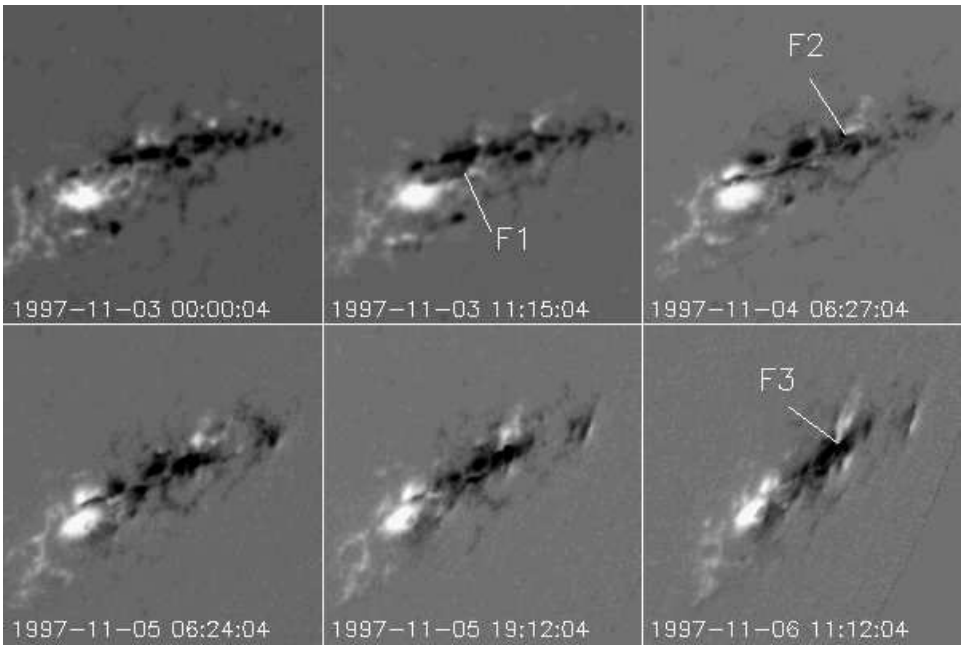

Figure 1. Evolution of magnetic field of the active region AR8100 from 1997 November 3 to 6. The marks 'F1', 'F2', and 'F3' denote the locations of the M4.2, X2.1/2B and X9.4/2B flares.

ary integral equation representation proposed by Yan and Sakurai (2000). The vector magnetic field data used here was taken at 00:56UT of November 4 at Huairou Solar Observing Station. Selected field lines, exhibiting basic magnetic configuration of the active region, are presented in Figure 2. Two bipolar magnetic configurations, shown in white and black lines respectively, are seen clearly. Both bipolar fields obey Hale-Nicholson polarity law (Hale & Nicholson, 1938). The small one is related to the positive magnetic feature mentioned above. Flares X2.1/2B and X9.4/2B (marked by "F2 & F3" in the left panel of Figure 2) occurred at the interface of the two bipolar magnetic fields. Flare M4.2 (marked by "F1" in Figure 2), on the other hand, occurred beneath the large bipolar field, far from the interface.

Thus, it is shown that, although the flares occurred in the active region AR8100 and were also associated with full halo CMEs, their geoeffectiveness is different (see Table 1). Only the X2.1/2B and X9.4/2B flares, which occurred at the same location, were associated with geomagnetic storms. It seems to suggest that the magnetic fields involved actually in the related flares play a role for occurrences of geomagnetic storms.

3.2. Active Region AR8375

Three flares in the active region AR8375, C5.2/SF at 03:14UT of 1998 November 4, C5.4/SF flare at 02:59UT of 1998 November 5, and M8.4/2B flare at 19:31UT of 1998 November 5, are associate with full halo CMEs. We mark the flares on the MDI magnetogram (see Figure 3) by "F1", "F2" and "F3". The magnetic

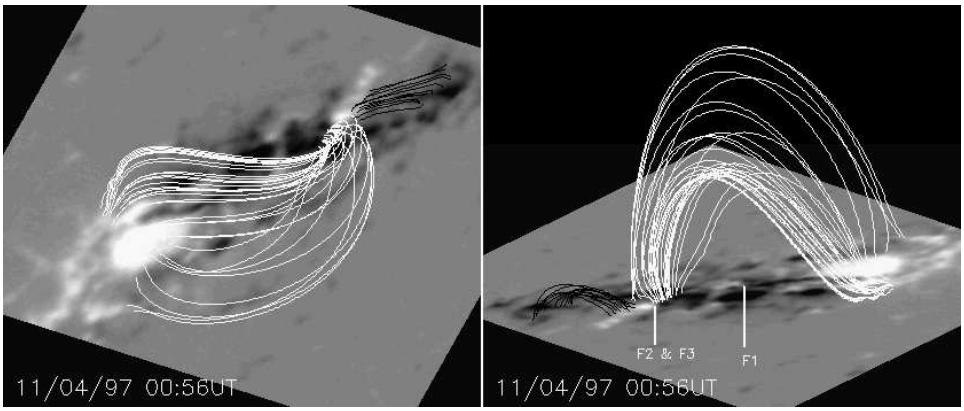

Figure 2. Selected field lines viewed from different angles show magnetic configuration in this active region. Apparently there are at least two well-defined bipolar magnetic configurations, as demonstrated in white field lines and black field lines, respectively. The X2.1/2B and X9.4/2B flares, marked by "F2 & F3", occurred at the interface of the two bipolar fields.

configuration of this active region appears fairly simple: a dominant spot with positive magnetic polarity sits at the center of the active region, surrounded by several small parasite negative magnetic features. The flares appear to be associated with three parasite features. The locations of these features are quite close. It is likely that these flares were triggered by the interaction of the small features and the major spot. We expect reasonably that the magnetic fields involved in those flares possess very similar configurations.

The flares are associated with full halo CMEs. All CMEs are found to produce geomagnetic storms (see Table 1).

3.3. Active Region AR9026

Active region AR9026 produced three flares (X2.3/3B flare at 12:06UT of 2000 June 6, X1.2/3B flare at 15:04UT of 2000 June 7, and X5.2/3B flare at 16:37UT of 2000 June 10), which are found to be associated with full halo CMEs. Again, we locate the flares on the corresponding magnetograms (see Figure 4). They are marked by 'F1', 'F2' and 'F3'. A time series of magnetograms in Figure 4 shows evolution of magnetic field of this region from June 6 to June 10, 2000. Significant change of magnetic field can be seen in this period: At the center of the images are two patches with opposite signs of magnetic polarity that decayed remarkably from June 6 to June 9, and are barely seen on June 10.

It is quite clear that the X2.3/3B and X1.2/3B flares occurred at the same place along the neutral line of the patches mentioned above. Although the third flare, F3, occurred geometrically close to this region, the basic configurations of magnetic fields in the region have changed: the two patches disappeared completely in the *MDI* 2000 June 10 16:00:03 magnetogram, before the X5.2/3B flare occurred.

It shows again that, although the three flares occurred in the same active region and were associated with full halo CMEs, only two flares, F1 and F2,

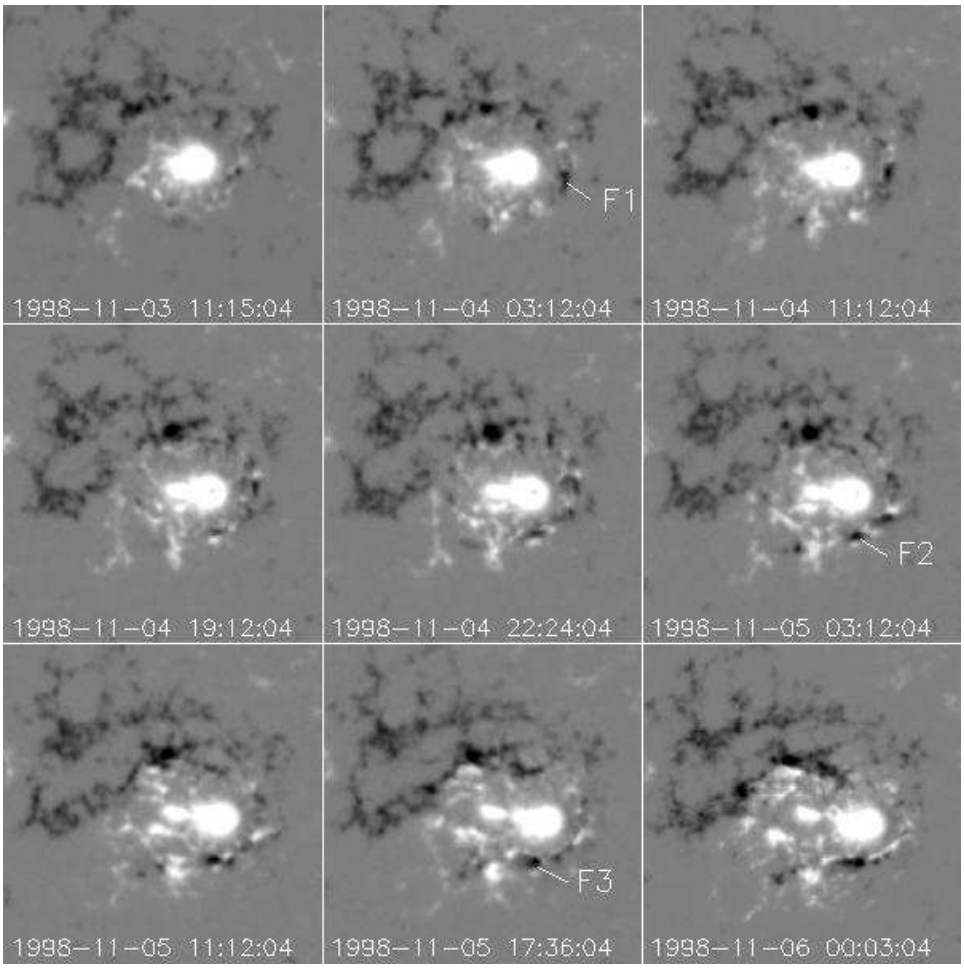

Figure 3. Evolution of magnetic field of the active region AR8375 from November 3 to November 6. The locations of the three flares are marked by 'F1', 'F2', and 'F3', respectively. It is seen that these locations are very close, and each one is associated spatially with a parasite magnetic feature surrounding the dominant magnetic patch at the center.

are found to be related to geomagnetic storms. They occurred at the neutral line of the major patches with opposite magnetic polarity signs. These patches disappeared before the third flare occurred.

4. Summary and Discussions

We have analyzed three active regions to explore relationship between magnetic structures of active regions and geomagnetic storms. Each active region is associated with multiple full halo CMEs. The full halo CMEs, though originated from the same active region, may not possess similar geoeffectiveness. We found that, when the associated flares occurred in the places where the configurations

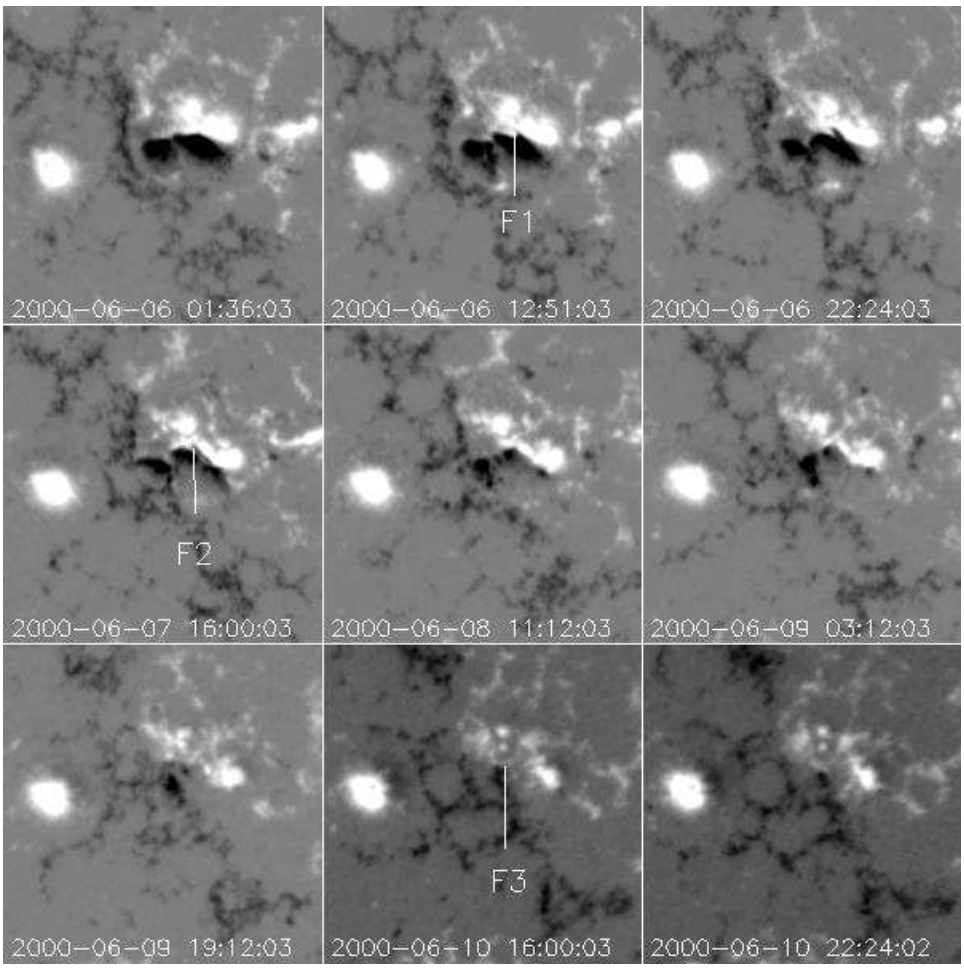

Figure 4. Evolution of magnetic field of the active region AR9026 from 2000 June 6 to June 10. In this period, three flares are found to be associated with full halo CMEs. The flares are denoted by 'F1', 'F2', and 'F3'. While the locations of the flares seem to be very close, the magnetic fields involved in the flares F1 and F2 are significantly different with those in the flare F3. The magnetic fields associated with the flares F1 and F2 completely disappeared when the flare F3 occurred. The CMEs related with F1 and F2 caused geomagnetic storms, but the one related with F3 didn't cause any storms.

of magnetic fields are identical or similar, the halo CMEs do intend to have similar geomagnetic effects. This implies that the flares, CMEs and geomagnetic storms are closely related magnetically in an intrinsic manner, as suggested by others (see, e.g. Webb et al. 2000, and references therein). This study also implies that the occurrences of solar active-region-related geomagnetic storms may not be determined by the active regions, but by the magnetic fields that are involved actually in the corresponding solar flare activities. This result agrees with what Leamon et al. (2002) found: the handedness of magnetic clouds asso-

ciated with sigmoid eruptions is only weakly related to their launch hemisphere, compared with a much strong correlation between magnetic clouds and eruptive filaments. Actually, the handedness of sigmoids is an average handedness of the whole active regions, not that of magnetic fields involved in the events.

The "conveyor belt" model, proposed by Chen (1989) (see also, Cliver & Hudson 2002), provides a theoretical interpretation for our results. In this model, a generic current sheet that has undergone the tearing mode instability and is consequently in a form of many intact flux ropes, emerges one-by-one from the convective zone to the solar atmosphere. The recurrence of flares and/or CMEs in essentially the same or close locations is a natural consequence of this model. Therefore the magnetic configurations involved in the events are very similar. If we believe that the solar-origin-geoeffectiveness is determined by the configurations of magnetic fields in the CMEs (see, e.g. Zhao, Hoeksema, & Marubashi 2001), the results in this study are easily understood.

Acknowledgments. We appreciate D. Zarro for the mapping software and the availability of the Solar SoftWare, which make the alignment much easier. We wish to thank D. Webb for providing data for the halo CMEs. Y Liu was supported at Stanford University by the NASA NAG5-13261, NSF/CISM project under grant ATM-0120950 and the DoD MURI grants. SOHO is a project of international cooperation between ESA and NASA.

References

Crooker, N. U. 2000, J. Atm. & Solar-Terres. Phys., 62, 1071
Chen, J. 1989, ApJ, 338, 453
Cliver, E. W., & Hudson, H. S. 2001 J. Atm. & Solar-Terres. Phys., 64, 231
Hale, G. E., & Nicholson, S. B. 1938, Magnetic Observationsof Sunspots, 1917-1924 (Washington, D.C: Carnegie institution of Washington)
Leamon, R. J., Canfield, R. C., & Pevtsov, A. A. 2002, JGR, 107, 1234
Liu, Y., Zhao, X., Hoeksema, J. T., Scherrer, P. H., Wang, J., & Yan, Y. 2002, Solar Phys., 206, 333
Pevtsov, A. A., & Canfield, R. C. 2001, JGR, 106, 25191
Titov, V. S., & Demoulin, P. 1999, A&A, 351, 707
Webb, D. F. et al. 2004, in preparation
Webb, D. F., Crooker, N. U., Plunkett, S. P., & St. Cyr, O. C. 2001, in Geophysics Monograph Ser. 125, Space Weather, ed. Song, P., Siscoe, G., & Singer, H., 123
Webb, D. F., Cliver, E. W., Crooker, N. U., St. Cyr, O. C., & Thompson, B. J. 2000, JGR, 105, 7491
Yan, Y., & Sakurai, T. 2000, Solar Phys., 195, 89
Yurchyshyn, V. B., Wang, H., Goode, P. R., & Deng, Y. 2001, ApJ, 563, 381
Zhang, J., Dere, K. P., Howard, R. A., & Bothmer, V. 2003, ApJ, 582, 520
Zhang, J., Dere, K. P., Howard, R. A., Kundu, M. R. & White, S. 2001, ApJ, 559, 452
Zhao, X., Hoeksema, J. T., & Marubashi, K. 2001, JGR, 106, 15643